

Interface metallic states between a topological insulator and a ferromagnetic insulator

Tetsuro Habe¹ and Yasuhiro Asano^{1,2}¹*Department of Applied Physics, Hokkaido University, Sapporo 060-8628, Japan*²*Center for Topological Science and Technology, Hokkaido University, Sapporo 060-8628, Japan*

(Received 25 April 2012; published 29 May 2012)

We study electronic structures at an interface between a topological insulator and a ferromagnetic insulator by using a three-dimensional two-band model. In usual ferromagnetic insulators, the exchange potential is much larger than the bulk gap size in the topological insulators and electronic structures are asymmetric with respect to the Fermi level. In such situation, we show that unusual metallic states appear under the magnetic moment pointing the perpendicular direction to the junction plane, which cannot be described by the two-dimensional effective model around the Dirac point. When the magnetic moment is in the parallel direction to the plane, the number of Dirac cones becomes even integers. The conclusions obtained in analytical calculations are confirmed by numerical simulations on tight-binding lattice.

DOI: [10.1103/PhysRevB.85.195325](https://doi.org/10.1103/PhysRevB.85.195325)

PACS number(s): 73.20.-r, 75.70.-i, 85.75.-d

I. INTRODUCTION

Physics of a metallic state on a surface of a three-dimensional (3D) topological insulator (TI)¹⁻⁴ is undoubtedly a hot issue these days.⁵⁻⁷ Intrinsic phenomena originated from the topological nature of the insulating state would open a novel field of condensed matter physics. In particular, the metallic surface state shows interesting features when the TI is attached to another materials with gapped excitation spectra such as superconductors⁸⁻¹⁰ and ferromagnetic insulators.¹¹⁻¹⁶ The existence of Majorana fermions has been discussed in hybrid structures of such materials.^{8,11,17-19}

The surface metallic state has a linear dispersion, so-called two-dimensional Dirac cone. The upper and lower corners touch at a point in Brillouin zone, so-called Dirac point. The 3D TI's can be classified into the strong and weak TI in terms of the number of Dirac points.^{1,3,20,21} Namely, the metallic state is protected from the impurity scattering for odd number Dirac cones,^{20,22} whereas it disappears for even number Dirac cones. To discuss intrinsic phenomena of TI's, it is necessary to tune the Fermi level near the Dirac point, which is possible in experiments by chemical doping.^{23,24}

At the interface of a TI and a ferromagnetic insulator (FI), the metallic state is drastically modified depending on the direction of magnetic moment.¹¹ The metallic state becomes insulating in the presence of magnetic moment perpendicular to the interface plane. On the other hand, it remains metallic in the presence of magnetic moment parallel to the interface. The parallel magnetic moments only shift the Dirac point from the Γ point in the Brillouin zone to another points there. Such conclusions have been obtained by analyzing effective theoretical model around the Dirac point, where the surface state is described by the two-dimensional Dirac Hamiltonian under the small exchange potential due to the magnetic moment. However it is unclear if these conclusions are still valid or not in real TI/FI junctions because the exchange potential of FI is much larger than the gap of TI.

In this paper, we study electronic states at the interface of FI/TI junction by using three-dimensional two-band model. We show that asymmetry of the band structure in FI with respect to the Fermi level separates the dispersion of interface state from bulk band in whole Brillouin zone. This suggests

that the effective theory around the Dirac point is no longer valid in real TI/FI junctions. A metallic interface state appears even when the magnetic moment in FI is perpendicular to the junction plane. When the magnetic moment in FI is parallel to the interface plane, number of Dirac points should be even number in whole Brillouin zone. In addition to large asymmetry of band structure in FI, breaking down the time-reversal symmetry and a basic feature of Brillouin zone also play important roles in there electric properties of the interface state. The conclusions obtained by analytical calculation are confirmed by numerical simulation on three-dimensional two-band tight-binding lattice. Obtained results would be important not only in the basic physics but also in the view of potential application.

This paper is organized as follows. In Sec. II, we summarize electric property at a TI/FI junction interface based on the effective Hamiltonian around the Dirac point. At the same time, we discuss the limits of the effective theory. In Sec. III, we analytically study effects of large band asymmetry and large magnetic moment of FI on the interface electric states. In Sec. IV, the conclusions based on the analytical results are checked by the numerical simulation on three-dimensional tight-binding model. The conclusion is given in Sec. V.

II. EFFECTIVE THEORY AROUND THE DIRAC POINT

We firstly summarize the features of the interface state which have been discussed by using effective Hamiltonian around the Dirac point in two dimensions.^{1,3} The effective Hamiltonian in two dimensions is derived from the three-dimensional electric states of a TI described by

$$H = \begin{pmatrix} A\hat{s}_0 & \mathbf{d}(\mathbf{k}) \cdot \hat{\mathbf{s}} \\ \mathbf{d}(\mathbf{k}) \cdot \hat{\mathbf{s}} & -A\hat{s}_0 \end{pmatrix}, \quad (1)$$

$$A = M_0 - \sum_{\alpha} B_{\alpha} k_{\alpha}^2, \quad (2)$$

where M_0 and B_{α} for $\alpha = 1-3$ are band parameters. The unit matrix in spin space is denoted by \hat{s}_0 and \hat{s}_{α} for $\alpha = 1-3$ are the Pauli matrices. The spin-orbit coupling is symbolically expressed by $\mathbf{d}(\mathbf{k})$, which satisfies

$$\mathbf{d}(-\mathbf{k}) = -\mathbf{d}(\mathbf{k}). \quad (3)$$

The surface state on the TI is approximately described by the effective Hamiltonian in two dimensions:

$$h_{\text{sur}}(k_x, k_y) = v_F \mathbf{D} \cdot \hat{\mathbf{s}} - \mu, \quad (4)$$

where v_F is the Fermi velocity. In what follows, we implicitly consider Bi_2Se_3 .⁵ However, the arguments below are valid for all TI's. For Bi_2Se_3 , it is shown that $\mathbf{D} = (-k_y, k_x)$.²⁵ The Dirac point is at $(k_x, k_y) = (0, 0)$, which we call Λ_0 in this paper. The dispersion relation becomes $E_k = v_F |\mathbf{k}| - \mu$. The spin configuration on the Fermi surface is schematically illustrated in Fig. 1(a), where we assume $\mu > 0$ and focus only on the upper Dirac cone. The direction of spin and that of momentum are locked to each other. Thus the spin direction flips abruptly at Λ_0 when we trace the electronic states along the line L as shown in Fig. 1(b). Thus the Dirac point may be a kink for the spin polarization on a line passing through it. This fact limits the validity of the effective theory around the Dirac point. Namely, it is impossible to extend the effective theory to electric states in whole Brillouin zone. Let us trace electronic states along the straight line between $\Lambda_1 = (\pi, 0)$ and $\Lambda'_1 = (-\pi, 0)$ in the upper Dirac cone. The states at Λ_1 and that at Λ'_1 must be identical to each other because the two points are connected by a reciprocal vector. In other words, the topology of the Brillouin zone is the same as that of two-dimensional torus ($T^2 = S^1 \times S^1$). Although the energy of the two states are equal to each other, the spin direction of the two states are opposite to each other. In the effective theory, Λ_1 and Λ'_1 characterize the different electronic states. In real TI's, the effective theory usually works well because electric states on the Dirac cone is absorbed into the bulk energy bands before $|\mathbf{k}|$ reaching at the zone boundary.

The interface state between a TI and a FI is also approximately described by the effective Hamiltonian around the Dirac point in two dimension:

$$h_{\text{TIFI}}(k_x, k_y) = h_{\text{sur}}(k_x, k_y) + \mathbf{M} \cdot \hat{\mathbf{s}} \quad (5)$$

where \mathbf{M} is the exchange potential in FI. Effects of the FI on the interface state are considered only through \mathbf{M} . It is easy to show that the magnetic moment perpendicular to the two-dimensional plane, M_z , gives rise to a gap energy at the Λ_0 . The magnetic moment parallel to the interface ($M_x, M_y, 0$), on the other hand, shifts the Dirac point from Λ_0 to $(M_y/v_F, -M_x/v_F)$. In addition to this, the Fermi level stays at the Dirac point even in the presence of $(M_x, M_y, 0)$.¹¹ The conclusions obtained by analyzing Eq. (5) seem to be valid for weak exchange potentials smaller than the gap size of TI.

However, the typical gap size in TI is 100 meV,^{4,26,27} whereas the gap of FI is of the order of eV.^{28–31} Thus the low-energy electronic states around the gap of TI should be studied by using more realistic theoretical model.

III. EFFECTS OF BAND ASYMMETRY AND LARGE MAGNETIC MOMENT OF TI

Let us consider a TI in three dimension under the exchange potential due to the magnetic moment in a FI. The Hamiltonian reads

$$H = \begin{pmatrix} h_0 \hat{s}_0 & \mathbf{d}(\mathbf{k}) \cdot \hat{\mathbf{s}} \\ \mathbf{d}(\mathbf{k}) \cdot \hat{\mathbf{s}} & -h_0 \hat{s}_0 \end{pmatrix}, \quad (6)$$

$$h_0 = M_0 - B_1 k_z^2 - B_2 (k_x^2 + k_y^2), \quad (7)$$

$$\mathbf{d}(\mathbf{k}) = (A_2 k_x, A_2 k_y, A_1 k_z), \quad (8)$$

where M_0 , A_1 , A_2 , B_1 , and B_2 are material parameters.²⁶ The wave number in x , y , and z directions are denoted by k_x , k_y , and k_z , respectively. The Hamiltonian (6) is decomposed into two parts:

$$H = H_0 + H', \quad (9)$$

$$H_0 = \begin{pmatrix} (M_0 - B_1 k_z^2) \hat{s}_0 & A_1 k_z \hat{s}_z \\ A_1 k_z \hat{s}_z & -(M_0 - B_1 k_z^2) \hat{s}_0 \end{pmatrix}, \quad (10)$$

$$H' = \begin{pmatrix} -B_2 (k_x^2 + k_y^2) \hat{s}_0 & A_2 (k_x \hat{s}_x + k_y \hat{s}_y) \\ A_2 (k_x \hat{s}_x + k_y \hat{s}_y) & B_2 (k_x^2 + k_y^2) \hat{s}_0 \end{pmatrix}. \quad (11)$$

To analyze interface electric state, we apply the transformation $k_z \rightarrow i\kappa$ in H_0 ,

$$H_0 = \begin{pmatrix} (M_0 + B_1 \kappa^2) \hat{s}_0 & i A_1 \kappa \hat{s}_z \\ i A_1 \kappa \hat{s}_z & -(M_0 + B_1 \kappa^2) \hat{s}_0 \end{pmatrix}. \quad (12)$$

In Fig. 1(c), schematic band structures of Europium chalcogenides are illustrated. The band structures are generally asymmetric with respect to the Fermi level in these materials, which we consider through two parameters M_1 and M_2 with $M_1 \neq M_2$ as shown in Fig. 1(c). The horizontal line shows the Fermi energy of FI. The lowest band and the highest one are spin splitted due to the exchange potential. We assume that the middle bands are spin degenerate. We consider the large asymmetry of the band structures through the the exchange

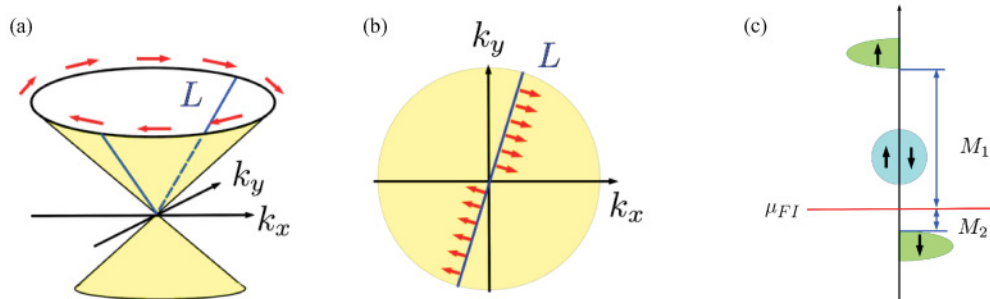


FIG. 1. (Color online) (a) The spin configuration of the Fermi surface. (b) The spin configuration on the line L . (c) The schematic band structure of a ferromagnetic insulator. The arrow in a band denotes spin direction and the horizontal line shows the Fermi energy.

Hamiltonian

$$H_m = \begin{pmatrix} M\hat{s}_\alpha + \mu_m\hat{s}_0 & 0 \\ 0 & 0 \end{pmatrix}, \quad (13)$$

$$M_1 = M + \mu_m, \quad M_2 = M - \mu_m, \quad (14)$$

where α indicates the direction of the magnetic moment in FI and μ_m represents the asymmetry in the band structure. In these definition, $M_1 = M_2$ and $M_1 \neq M_2$ describe the symmetric and asymmetric band structures, respectively. We assume that the correction for Hamiltonian of surface state in TI has same manner.

A. Perpendicular magnetic moment to plane

When the magnetic moment of FI is perpendicular to the junction plane, the exchange Hamiltonian for the surface state is

$$H_m = \begin{pmatrix} M_1 & 0 & 0 & 0 \\ 0 & -M_2 & 0 & 0 \\ 0 & 0 & 0 & 0 \\ 0 & 0 & 0 & 0 \end{pmatrix}. \quad (15)$$

In usual FI's, a relation $M_i \gg M_0$ holds. The Hamiltonian $H_0 + H_m$ is decomposed into two 2×2 matrices whose eigenvalues are $E_i = (\tilde{M}_i - M_0)/2$ with $\tilde{M}_1 = M_1 + M_0$ and $\tilde{M}_2 = -M_2 + M_0$. The eigenstates of can be expressed by

$$\mathbf{v}_1(\kappa_1) = \begin{pmatrix} a_1(\kappa_1) \\ 0 \\ b_1(\kappa_1) \\ 0 \end{pmatrix}, \quad \mathbf{v}_2(\kappa_2) = \begin{pmatrix} 0 \\ a_2(\kappa_2) \\ 0 \\ b_2(\kappa_2) \end{pmatrix}. \quad (16)$$

The coefficients a_i and b_i satisfy

$$\frac{a_i}{b_i} = -\frac{i D_i \kappa}{(\tilde{M}_i + M_0)/2 - B_1 \kappa^2}, \quad (17)$$

where $D_1 = A_1$ and $D_2 = -A_1$. This Hamiltonian is equivalent to that of the surface state of a TI facing to vacuum by substituting $(\tilde{M}_i + M_0)/2$ by M_0 .

The imaginary wave number κ_i^\pm takes different forms depending on the sign of $\tilde{M}_i + M_0$. For $\tilde{M}_i + M_0 > 0$, κ has the similar form as it is in the TI/vacuum surface,

$$\kappa_i^\pm = \frac{A_1}{2B_1} \left(1 \pm \sqrt{1 - \frac{2B_1(\tilde{M}_i + M_0)}{A_1^2}} \right). \quad (18)$$

The eigenstate in this case can be described by

$$\begin{pmatrix} a_i \\ b_i \end{pmatrix} = \begin{pmatrix} D_i/A_1 \\ i \end{pmatrix} (C_+ e^{-\kappa_i^+ z} + C_- e^{-\kappa_i^- z}), \quad (19)$$

with C_\pm being arbitrary constants. For $\tilde{M}_i + M_0 < 0$, the wave number becomes

$$\kappa_i^\pm = \frac{A_1}{2B_1} \left(\sqrt{1 - \frac{2B_1(\tilde{M}_i + M_0)}{A_1^2}} \pm 1 \right). \quad (20)$$

The eigenstate is given by

$$\begin{pmatrix} a_i \\ b_i \end{pmatrix} = C_+ \begin{pmatrix} D_i/A_1 \\ i \end{pmatrix} e^{-\kappa_i^+ z} + C_- \begin{pmatrix} -D_i/A_1 \\ i \end{pmatrix} e^{-\kappa_i^- z}. \quad (21)$$

For $M_1 > 0$, $\tilde{M}_1 + M_0 > 0$ always holds. Thus κ_1 takes Eq. (18). On the other hand, $\tilde{M}_1 + M_0$ can be either positive or negative even for $M_2 > 0$.

We first analyze weak exchange potential satisfying $M_2 < 2M_0$. The wave function of in this case is

$$\begin{pmatrix} a_i \\ b_i \end{pmatrix} = \begin{pmatrix} D_i/A_1 \\ i \end{pmatrix} [C_i^+ \exp(-\kappa_i^+ z) + C_i^- \exp(-\kappa_i^- z)], \quad (22)$$

with C_i^\pm being the normalization constant. For simplicity, in what follows, we drop z dependence from the wave function. There are only two independent wave function for $M_2 < 2M_0$. The surface state is a superposition of ψ_1 and ψ_2 that are defined by

$$\psi_1 = \frac{1}{\sqrt{2}} \begin{pmatrix} 1 \\ 0 \\ i \\ 0 \end{pmatrix}, \quad \psi_2 = \frac{1}{\sqrt{2}} \begin{pmatrix} 0 \\ -1 \\ 0 \\ i \end{pmatrix}. \quad (23)$$

The total Hamiltonian $H_0 + H' + H_m$ can be represented in this basis of ψ_i as

$$H = \begin{pmatrix} M_1 & 0 \\ 0 & -M_2 \end{pmatrix} + \begin{pmatrix} H'_{11} & H'_{12} \\ H'_{21} & H'_{22} \end{pmatrix} = \begin{pmatrix} M_1 & i v_F(k_x - i k_y) \\ -i v_F(k_x + i k_y) & -M_2 \end{pmatrix}, \quad (24)$$

$$H'_{ij} = \langle \psi_i | H' | \psi_j \rangle \quad (25)$$

with $v_F = A_2$. The energy of the surface state is

$$E = \frac{M_1 - M_2}{2} \pm \sqrt{\frac{(M_1 + M_2)^2}{4} + v_F^2 k^2} \quad (26)$$

with $k = \sqrt{k_x^2 + k_y^2}$. For weak exchange potential $M_2 < 2M_0$, the exchange potential in the z direction causes the gap, which is consistent with the previous theories.¹¹ The asymmetry of the band structures gives a constant energy shift to the dispersion relation.

Next, we consider strong exchange potential satisfying $M_2 > 2M_0$. In this case, the straightforward calculation of the eigenfunction at the Γ point results in

$$\psi_1 = \frac{1}{\sqrt{2}} \begin{pmatrix} 1 \\ 0 \\ i \\ 0 \end{pmatrix}, \quad \psi_2 = \frac{1}{\sqrt{2}} \begin{pmatrix} 0 \\ 1 \\ 0 \\ i \end{pmatrix}, \quad \psi_3 = \frac{1}{\sqrt{2}} \begin{pmatrix} 0 \\ -1 \\ 0 \\ i \end{pmatrix}. \quad (27)$$

For convenience, we employ another basis as follows:

$$\psi'_1 = \frac{1}{\sqrt{2}} \begin{pmatrix} 1 \\ 0 \\ i \\ 0 \end{pmatrix}, \quad \psi'_2 = \begin{pmatrix} 0 \\ 1 \\ 0 \\ 0 \end{pmatrix}, \quad \psi'_3 = \begin{pmatrix} 0 \\ 0 \\ 0 \\ 1 \end{pmatrix}. \quad (28)$$

The total Hamiltonian $H_0 + H' + H_m$ in this representation reads

$$H = \begin{pmatrix} M_1 & -i v_F(k_x - i k_y) & v_F(k_x - i k_y) \\ i v_F(k_x + i k_y) & -M_2 - B_2 k^2 & 0 \\ v_F(k_x + i k_y) & 0 & -M_2 + B_2 k^2 \end{pmatrix}. \quad (29)$$

with $v_F = A_2/\sqrt{2}$. The energy dispersion can be derived from the eigenequation

$$x^3 - 2Mx^2 - (B_2^2k^4 + 2v_F^2k^2)x + 2MB_2^2k^4 = 0, \quad (30)$$

with $x = E + M_2$. At the vicinity of Γ point, $x(k)$ is approximately given by

$$x(k) = a_0 + a_1k^2 + a_2k^4. \quad (31)$$

Here, a_0 can be obtained easily by putting $k = 0$. We obtain two values:

$$a_0 = 0, \quad 2M. \quad (32)$$

For $a_0 = 0$, a_i can be derived by putting the coefficients of k^4 and k^6 terms in Eq. (30) to be zero. Since $M \gg M_0$, a_1 and a_2 have simple expression

$$a_1 = -\frac{v_F^2}{2M} \pm B_2 \sqrt{1 + \frac{v_F^4}{4M^2 B_2^2}} \quad (33)$$

$$\simeq -\frac{v_F^2}{2M} \pm B_2, \quad (34)$$

$$a_2 \simeq \mp \frac{v_F^2}{4M^2} B_2. \quad (35)$$

Then the energy dispersions are approximately given by

$$E(k) = -M_2 \pm B_2k^2 \mp \frac{v_F^2}{4M^2} B_2k^4. \quad (36)$$

In the same way, we also obtain

$$E(k) = M_1 + \frac{v_F^2}{M}k^2 - \frac{v_F^4}{2M^3}k^4, \quad (37)$$

for $a_0 = 2M$. For both $a_0 = 0$ and $2M$, the coefficient of k^2 and that of k^4 have opposite sign to each other. In addition, we can also predict that two minima of the dispersion go across the Fermi level and the interface becomes metallic for $M > 2M_0$.

B. Parallel magnetic moment to plane

When the magnetic moment of FI is parallel to the junction plane, the Hamiltonian of the surface state at Γ point is $H_0 + H_m$ with

$$H_m = \begin{pmatrix} M\hat{s}_x + \mu_m\hat{s}_0 & 0 \\ 0 & 0 \end{pmatrix}. \quad (38)$$

Here, we assume that the magnetic moment is in the x direction. This does not lose the generality of argument below because the Hamiltonian is rotationally invariant in momentum space. Applying a unitary transformation, we obtain

$$U^\dagger(H_0 + H_m)U = \begin{pmatrix} (M_0 + B_1\kappa^2)\hat{s}_0 + \hat{M} & -iA_1\kappa s_x \\ -iA_1\kappa s_x & -(M_0 + B_1\kappa^2)\hat{s}_0 \end{pmatrix}, \quad (39)$$

$$\hat{M} = \begin{pmatrix} M_1 & 0 \\ 0 & -M_2 \end{pmatrix}, \quad (40)$$

with

$$U = \begin{pmatrix} (\hat{s}_0 - i\hat{s}_y)/\sqrt{2} & 0 \\ 0 & (\hat{s}_0 + i\hat{s}_y)/\sqrt{2} \end{pmatrix}. \quad (41)$$

The eigenvectors can be expressed by

$$\psi_1 = \begin{pmatrix} a_1(\kappa) \\ 0 \\ 0 \\ b_1(\kappa) \end{pmatrix}, \quad \psi_2 = \begin{pmatrix} 0 \\ a_2(\kappa) \\ b_2(\kappa) \\ 0 \end{pmatrix}. \quad (42)$$

The elements satisfy

$$\frac{a_i}{b_i} = \frac{iA_1\kappa}{\tilde{M}_i + B_1\kappa^2}, \quad (43)$$

where $\tilde{M}_1 = M_0 + M$ and $\tilde{M}_2 = M_0 - M$. The eigenvalues and eigenvectors can be calculated in the same way with the previous section.

When the exchange potential is weak $M_2 < 2M_0$, the eigenvectors are the eigenvalues E_i are

$$E_1 = \frac{M_1}{2}, \quad E_2 = -\frac{M_2}{2}. \quad (44)$$

Corresponding vectors are given by

$$\psi_1 = \frac{1}{\sqrt{2}} \begin{pmatrix} -1 \\ 0 \\ 0 \\ i \end{pmatrix}, \quad \psi_2 = \frac{1}{\sqrt{2}} \begin{pmatrix} 0 \\ -1 \\ i \\ 0 \end{pmatrix}. \quad (45)$$

The total Hamiltonian $H = \tilde{H}_0 + U^\dagger H' U$ becomes

$$H = \frac{M_1 - M_2}{2} s_0 + \begin{pmatrix} M - v_F k_y & -i v_F k_x \\ i v_F k_x & -M + v_F k_y \end{pmatrix}, \quad (46)$$

where $v_F = A_2$ and $2M = M_1 + M_2$. The energy dispersion is given by

$$E = \frac{M_1 - M_2}{2} \pm v_F \sqrt{k_x^2 + (k_y - M/v_F)^2}. \quad (47)$$

The Dirac point moves from the Γ point to $(0, M)$, which is consistent with the effective theory in around the Dirac point. The asymmetry of the band structures, however, shifts the Fermi level from the Dirac point.

When the exchange potential is sufficiently large satisfying $M_2 > 2M_0$, the basis of the surface state becomes

$$\psi_1 = \frac{1}{\sqrt{2}} \begin{pmatrix} -1 \\ 0 \\ 0 \\ i \end{pmatrix}, \quad \psi_2 = \begin{pmatrix} 0 \\ 1 \\ 0 \\ 0 \end{pmatrix}, \quad \psi_3 = \begin{pmatrix} 0 \\ 0 \\ 1 \\ 0 \end{pmatrix}. \quad (48)$$

The total Hamiltonian $H = H_0 + H' + H_m$ in this basis results in

$$H = \begin{pmatrix} M_1 - v_F k_y & -i v_F k_x/\sqrt{2} & -v_F k_x/\sqrt{2} \\ i v_F k_x/\sqrt{2} & -M_2 + B_2 k^2 & i v_F k_y \\ -v_F k_x/\sqrt{2} & -i v_F k_y & -M_2 - B_2 k^2 \end{pmatrix}, \quad (49)$$

with $v_F = A_2$.

By analyzing Eq. (49) in detail, we can conclude that (a) there are two Dirac cones in the whole Brillouin zone, (b) the asymmetry of band structure in FI with respect to the Fermi level may causes the separation of the interface state from the bulk band, and (c) three branches of surface states appear in the gap of TI. These conclusions can be confirmed in a simple case where we consider the dispersion relation along a line satisfying $k_x = 0$. At $k_x = 0$, three dispersion branches appear

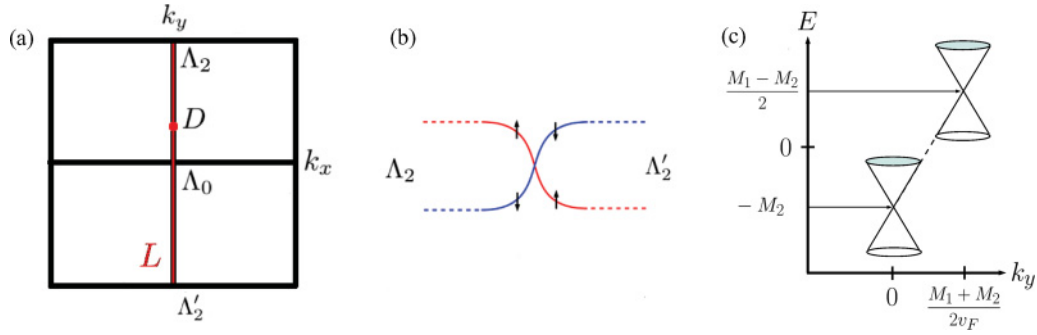


FIG. 2. (Color online) (a) The simple Brillouin zone and its TRI points Λ_i . In this figure, Λ_2 and Λ'_2 are same TRI points under translational operation of a reciprocal lattice vector. (b) The spin configuration on the line L with a single Dirac points is illustrated. (c) In the parallel magnetic moment case, the positions of two Dirac cones are shown.

at the interface

$$E_1 = M_1 - v_F k_y, \quad (50)$$

$$E_2 = -M_2 - v_F k_y \sqrt{1 + (B_2^2/v_F^2)k_y^2}, \quad (51)$$

$$E_3 = -M_2 + v_F k_y \sqrt{1 + (B_2^2/v_F^2)k_y^2}. \quad (52)$$

Near the Γ point, two branches E_1 and E_2 are almost parallel to each other. The remaining branch E_3 goes across E_1 and E_2 . Therefore there are two Dirac points. For $k'_y = k_y - (M_1 + M_2)/2v_F$, Eqs. (50) and (52) can be represented by

$$E = \frac{M_1 - M_2}{2} \pm v_F k'_y, \quad (53)$$

where higher order terms for k^3 in Eq (52) are ignored. The first term implies a asymmetry of the band structure of FI. Another Dirac point is obtained by Eqs. (51) and (52) in the same way:

$$E = -M_2 \pm v_F k_y, \quad (54)$$

where higher order terms for k^3 in Eqs. (51) and (52) are ignored. The schematic illustration for positions of two Dirac points is shown in Fig. 2(c).

As we have discussed above, the asymmetry of band structure in FI removes the dispersion of the interface state from the bulk band. This causes more drastic modification of interface state in the presence of magnetic moment parallel to the interface plane. When $\mathbf{M} = (M_x, 0, 0)$, the magnetic moment shifts the Dirac point from Λ_0 in the Brillouin zone to a point D as shown in Fig. 2(a). Let us consider the spin configuration along a line that satisfies $\mathbf{D} \parallel \mathbf{M}$ (Eq. (4) and passes through the Dirac point D . For $\mathbf{M} = (M_x, 0, 0)$, the line corresponds to the straight line L connecting Λ_2 and Λ'_2 as shown in Fig. 2(a). We note two key features of spin direction along the line: (i) Λ_2 and Λ'_2 are identical point to each other and (ii) the spin direction flips at D . If the number of the Dirac point is one, spin direction at Λ_2 and Λ'_2 would be opposite to each other. This statement, however, contradict to (i). Therefore the number of Dirac point must be an even integer on $\Lambda_2 - \Lambda'_2$. Since D is a Dirac point, at least one extra Dirac point is necessary on $\Lambda_2 - \Lambda'_2$ [see Fig. 2(b)].

This conclusion above can be obtained in more general argument. The Dirac point can be regarded as the magnetic monopole in the momentum space. The Gauss integration in

the first Brillouin zone becomes finite in the presence of the single monopole. This integration should coincide with the path integration of $\mathbf{D}(\mathbf{k})$ along the zone boundary. However, the integration along the boundary vanishes because of the relation $\mathbf{D}(-\mathbf{k}) = -\mathbf{D}(\mathbf{k})$. Thus there must be extra monopoles in the Brillouin zone. According to this argument, the number of the Dirac points must be even number in the Brillouin zone. In Eq. (52), two Dirac points are expected in the present situation. The conclusions obtained by the analytical calculation are confirmed by numerical simulation in the next section.

IV. NUMERICAL RESULTS IN 3D

Let us consider a junction of TI and FI on three-dimensional tight-binding lattice as shown in Fig. 3(a). We describe the TI by using the two-band model as

$$H_{\text{TI}} = \sum_{j,j'} \sum_{\mathbf{k}} [\tilde{c}_{\mathbf{k},j',1}^\dagger, \tilde{c}_{\mathbf{k},j',2}^\dagger] \begin{bmatrix} \xi_{\text{TI}} \hat{s}_0 & \mathbf{A} \cdot \hat{\mathbf{s}} \\ \mathbf{A} \cdot \hat{\mathbf{s}} & -\xi_{\text{TI}} \hat{s}_0 \end{bmatrix} \begin{bmatrix} \tilde{c}_{\mathbf{k},j,1} \\ \tilde{c}_{\mathbf{k},j,2} \end{bmatrix}, \quad (55)$$

$$\tilde{c}_{\mathbf{k},j,v} = \begin{bmatrix} c_{\mathbf{k},j,v,\uparrow} \\ c_{\mathbf{k},j,v,\downarrow} \end{bmatrix}, \quad (56)$$

$$\xi_{\text{TI}} = [M_0 - 2b_1 + 2b_2 \cos(k_x a) + 2b_2 \cos(k_y a) - 4b_2 - \mu_{\text{TI}}] \delta_{j,j'} + b_1 (\delta_{j,j'+1} + \delta_{j,j'-1}), \quad (57)$$

$$\mathbf{A} = [a_2 k_x \delta_{j,j}, a_2 k_y \delta_{j,j}, -i a_1 (\delta_{j,j'+1} - \delta_{j,j'-1})], \quad (58)$$

where $c_{\mathbf{k},j,\mu,s}^\dagger$ ($c_{\mathbf{k},j,\mu,s}$) is the creation (annihilation) operator of an electron with spin s , belonging to the band $\nu = 1-2$,

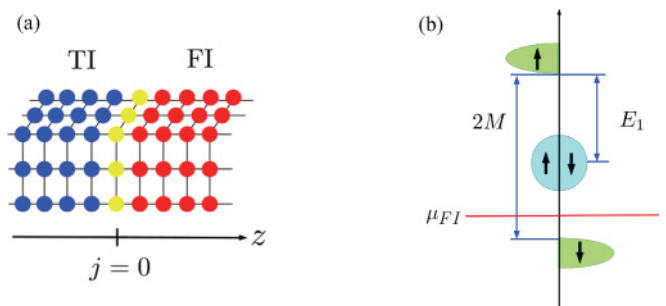


FIG. 3. (Color online) (a) TI/FI junction on the three-dimensional tight-binding lattice. The interface is at $j = 0$. (b) The schematic band structure of a FI. The arrow in a band denotes spin direction and the horizontal line labeled by ϵ_F is the Fermi energy.

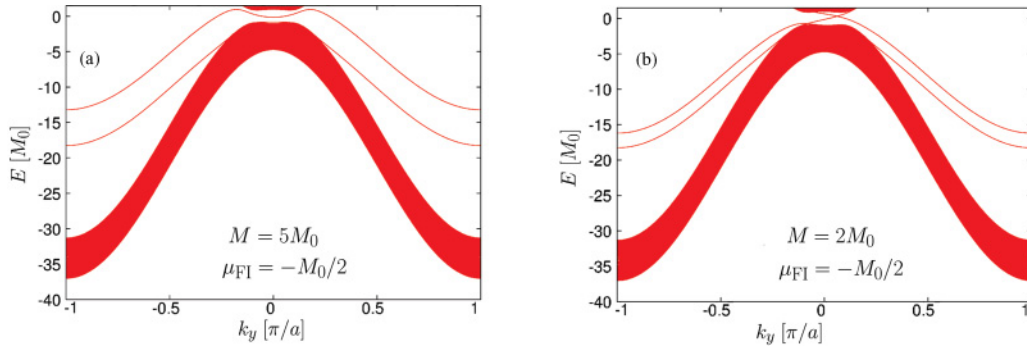


FIG. 4. (Color online) The global pictures of band structures are showed for a perpendicular (a) and a parallel (b) magnetic moments.

having two-dimensional wave vector $\mathbf{k} = (k_x, k_y)$, and at a lattice site $j < 0$ in the z direction. We used the periodic boundary condition in the xy plane.

In the same way, we describe the FI by

$$H_{\text{FI}} = \sum_{j,j'} \sum_{\mathbf{k}} [\tilde{c}_{\mathbf{k},j',1}^\dagger, \tilde{c}_{\mathbf{k},j',2}^\dagger] \times \begin{bmatrix} (\xi_{\text{FI}} + E_1)\hat{\delta}_0 & 0 \\ 0 & (-\xi_{\text{FI}} + E_2)\hat{\delta}_0 + \mathbf{M} \cdot \hat{\mathbf{s}} \end{bmatrix} \begin{bmatrix} \tilde{c}_{\mathbf{k},j,1} \\ \tilde{c}_{\mathbf{k},j,2} \end{bmatrix}, \quad (59)$$

$$\xi_{\text{FI}} = [2t \cos(k_x) + 2t \cos(k_y) - 8t - \mu_{\text{FI}}] \delta_{j,j'} + t(\delta_{j,j'+1} + \delta_{j,j'-1}), \quad (60)$$

for $j > 0$. At the interface ($j = 0$), TI and FI are connected by

$$H_I = \sum_{\mathbf{k}} [\tilde{c}_{\mathbf{k},0,1}^\dagger, \tilde{c}_{\mathbf{k},0,2}^\dagger] \times \begin{bmatrix} (\xi_I + E_1/2)\hat{\delta}_0 & \mathbf{A}' \cdot \hat{\mathbf{s}} \\ \mathbf{A}' \cdot \hat{\mathbf{s}} & (-\xi_I + E_2/2)\hat{\delta}_0 + \mathbf{M} \cdot \hat{\mathbf{s}}/2 \end{bmatrix} \times \begin{bmatrix} \tilde{c}_{\mathbf{k},0,1} \\ \tilde{c}_{\mathbf{k},0,2} \end{bmatrix}, \quad (61)$$

$$2\xi_I = M_0 - 2b_1 + 2(b_2 + t) \cos(k_x) + 2(b_2 + t) \cos(k_y) - 4b_2 - 8t - \mu_{\text{TI}} - \mu_{\text{FI}}, \quad (62)$$

$$2\mathbf{A}' = (a_2 k_x, a_2 k_y, 0). \quad (63)$$

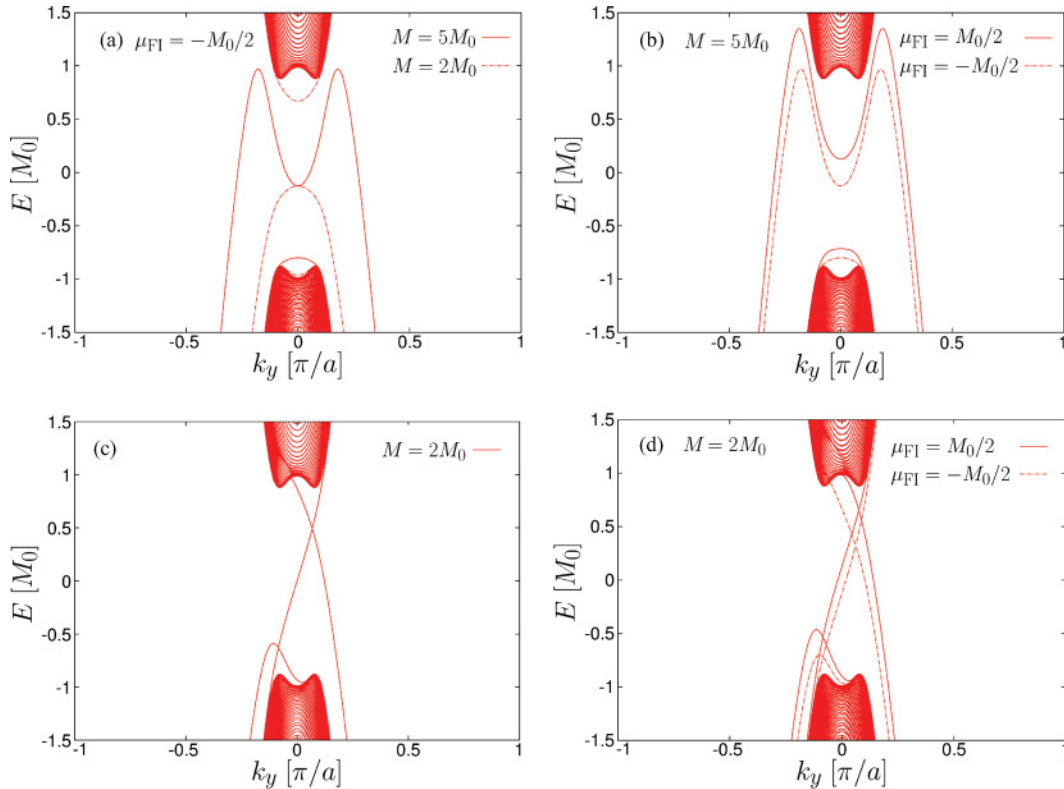


FIG. 5. (Color online) The band structures of TI/FI junction with a perpendicular (a) and (b) and parallel (c) and (d) magnetic moment are plotted of the energy E vs the wave vector k_y . The optical gap of FI is locked in $2M_0$ in (a) and (c). The magnitude of a magnetic moment of FI is $2M_0$ and $5M_0$. There are the surface band separated from the bulk band structure. The effect by shifting the Fermi energy in the optical gap is plotted in (b) and (d).

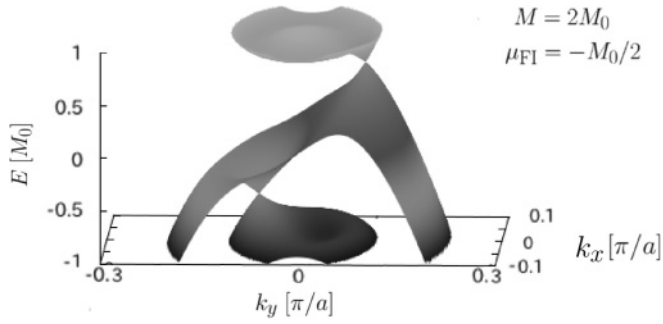


FIG. 6. The dispersion of the interface states in TI/FI junction with magnetic moment parallel to the interface are plotted in two-dimensional Brillouin zone. To show two Dirac point clearly, k_x is restricted within $[-10^{-1}\pi/a, 10^{-1}\pi/a]$.

The hard-wall boundary condition along with z axis is employed. The parameters in this calculation take values of Bi_2Se_3 : $a_1 = 7.86M_0/a$, $a_2 = 14.6M_0/a$, $b_1 = 3.57 \times 10M_0/a^2$, and $b_2 = 2.02 \times 10^2M_0/a^2$ in TI side.²⁶ The lattice constant a is about 5 \AA . In FI, we assume $b_{\text{FI}} = 10^{-2}b_1$ and $E_1 = -E_2 = -M/2$. The total lattice size in the z direction is 200 sites, where TI and FI occupy 150 and 50 sites, respectively. A schematic band picture of a FI is shown in Fig. 3(b). Electronic structure becomes asymmetric with respect to the Fermi level.

We first show the dispersion relations of the interface states rather large energy range for magnetic moment perpendicular to the interface [see Fig. 4(a)] and for magnetic moment parallel to the interface [see Fig. 4(b)], where the dispersion is calculated along $k_x = 0$, $\mu_{\text{FI}} = -M_0/2$, $M = 5M_0$ in (a) and $M = 2M_0$ in (b). The wave function of the interface states behaves like e^{j/j_0} for $j < 0$ in TI with j_0 being the inverse of localizing length. In the figures, we also show the bulk band in TI. As we discussed in Sec. III, the upper dispersion in (a) is clearly separated from the bulk band of TI in whole Brillouin zone because of the band asymmetry in FI. The dispersions of the interface states for the magnetic moment parallel to the interface have rather complicated structure as shown in (b). We note that upper dispersion branch is well separated from the bulk band for $|k_y| > 0.3$. We zoom up the dispersion relations near the Γ point and discuss their features in the next figures.

In Fig. 5(a), we show the dispersion relation of the interface states along $k_x = 0$ for the magnetic moment perpendicular to the interface. Here, we assume $\mu_{\text{FI}} = -M_0/2$ and show the results for $M = 2M_0$ and $5M_0$. When the magnetic moment is relatively small at $M = 2M_0$, the Dirac cone disappears as predicted by the effective theory around the Dirac point. When

we increase the exchange potential at $M = 5M_0$, however, the dispersion of the interface state behaves like $\epsilon_k \approx \alpha_0 - \alpha_2k^2 + \alpha_4k^4$. As a result, the interface states become metallic. Features of the metallic also depends on the Fermi level in the FI. The dispersion relation in Fig. 5(b) show that the number of Fermi surface is one for $\mu_{\text{FI}} = M_0/2$, whereas for $\mu_{\text{FI}} = -M_0/2$ two Fermi surface appears. These numerical results are consistent with analytical ones in Sec. III.

Next, we look into the interface states at TI/FI junction in the presence of the magnetic moment parallel to the junction plane. Figure 5(c) shows the dispersion relation along $k_x = 0$ for $M \parallel x$, where $\mu_{\text{FI}} = 0$ and $M = 2M_0$. There are two Dirac cones in the Brillouin zone, which is consistent with the argument in Sec. III. In Fig. 5(d), we show the results at $M = 2M_0$ for $\mu_{\text{FI}} = -M_0/2$ and $M_0/2$. The characteristic features of the interface states are insensitive to parameters such as μ_{FI} and M . Finally, we show the energy dispersion for $\mu_{\text{FI}} = -M_0/2$ and $M = 2M_0$ in two-dimensional Brillouin zone in Fig. 6(a). In this figure, it is clear that there are two Dirac points in two-dimensional Brillouin zone.

V. CONCLUSION

In this paper, we have studied electronic properties of interface state between a topological insulator (TI) and a ferromagnetic insulator (FI) by using two-band model in three-dimension in both analytically and numerically. The energy gap of FI is usually much larger than that of TI and the band structures in FI is asymmetric with respect to its Fermi level. The dispersion branches of the interface state are separated from the bulk band in whole Brillouin zone due to the asymmetry of the band structures. When the magnetic moment is in the perpendicular direction to the interface plane, the interface states become metallic. The number of Fermi surfaces of such interface states depends on the material parameters. When the magnetic moment is in the parallel direction to the interface plane, metallic states always appear irrespective of the amplitude of the exchange potential. The number of the Dirac point becomes even integers in whole Brillouin zone. Such drastic effects of the magnetic moment on interface states obtained in analytical calculation have been confirmed by the numerical simulation on the tight-binding lattice.

ACKNOWLEDGMENT

This work was supported by the ‘‘Topological Quantum Phenomena’’ (No. 22103002) Grant-in Aid for Scientific Research on Innovative Areas from the Ministry of Education, Culture, Sports, Science, and Technology (MEXT) of Japan.

¹L. Fu, C. L. Kane, and E. J. Mele, *Phys. Rev. Lett.* **98**, 106803 (2007).

²L. Fu and C. L. Kane, *Phys. Rev. B* **76**, 045302 (2007).

³J. E. Moore and L. Balents, *Phys. Rev. B* **75**, 121306 (2007).

⁴Y. L. Chen, J. G. Analytis, J.-H. Chu, Z. K. Liu, S. K. Mo, X. L. Qi, H. J. Zhang, D. H. Lu, X. Dai, Z. Fang, S. C. Zhang,

I. R. Fisher, Z. Hussain, and Z. X. Shen, *Science* **325**, 178 (2009).

⁵M. Z. Hasan and C. L. Kane, *Rev. Mod. Phys.* **82**, 3045 (2010).

⁶S. Murakami, R. Takahashi, O. A. Tretiakov, A. Abanov, and J. Sinova, *J. Phys.: Conf. Ser.* **334**, 012013 (2011).

⁷X. L. Qi and S. C. Zhang, *Rev. Mod. Phys.* **83**, 1057 (2011).

- ⁸L. Fu and C. L. Kane, *Phys. Rev. Lett.* **100**, 096407 (2008).
- ⁹T. D. Stanescu, J. D. Sau, R. M. Lutchyn, and S. Das Sarma, *Phys. Rev. B* **81**, 241310(R) (2010).
- ¹⁰M. Lababidi and E. Zhao, *Phys. Rev. B* **83**, 184511 (2011).
- ¹¹Y. Tanaka, T. Yokoyama, and N. Nagaosa, *Phys. Rev. Lett.* **103**, 107002 (2009).
- ¹²A. A. Burkov and D. G. Hawthorn, *Phys. Rev. Lett.* **105**, 066802 (2010).
- ¹³T. Yokoyama, Y. Tanaka, and N. Nagaosa, *Phys. Rev. B* **81**, 121401(R) (2010).
- ¹⁴T. Yokoyama, J. Zang, and N. Nagaosa, *Phys. Rev. B* **81**, 241410(R) (2010).
- ¹⁵I. Garate and M. Franz, *Phys. Rev. Lett.* **104**, 146802 (2010).
- ¹⁶K. Nomura and N. Nagaosa, *Phys. Rev. B* **82**, 161401 (2010).
- ¹⁷A. R. Akhmerov, J. Nilsson, and C. W. J. Beenakker, *Phys. Rev. Lett.* **102**, 216404 (2009).
- ¹⁸J. Linder, Y. Tanaka, T. Yokoyama, A. Sudbo, and N. Nagaosa, *Phys. Rev. Lett.* **104**, 067001 (2010).
- ¹⁹Y. L. Chen, J.-H. Chu, J. G. Analytis, Z. K. Liu, K. Igarashi, H.-H. Kuo, X. L. Qi, S. K. Mo, R. G. Moore, D. H. Lu, M. Hashimoto, T. Sasagawa, S. C. Zhang, I. R. Fisher, Z. Hussain, and Z. X. Shen, *Science* **329**, 659 (2010).
- ²⁰P. Roushan, J. Seo, C. V. Parker, Y. S. Hor, D. Hsieh, D. Qian, A. Richardella, M. Z. Hasan, R. J. Cava, and A. Yazdani, *Nature (London)* **460**, 1106 (2009).
- ²¹T. Zhang, P. Cheng, X. Chen, J. F. Jia, X. Ma, K. He, L. Wang, H. Zhang, X. Dai, Z. Fang, X. Xie, and Q. K. Xue, *Phys. Rev. Lett.* **103**, 266803 (2009).
- ²²H. T. He, G. Wang, T. Zhang, I. K. Sou, G. K. L. Wong, J. N. Wang, H. Z. Lu, S. Q. Shen, and F. C. Zhang, *Phys. Rev. Lett.* **106**, 166805 (2011).
- ²³D. Hsieh, Y. Xia, D. Qian, L. Wray, J. H. Dil, F. Meier, J. Osterwalder, L. Patthey, J. G. Checkelsky, N. P. Ong, A. V. Fedorov, H. Lin, A. Bansil, D. Grauer, Y. S. Hor, R. J. Cava, and M. Z. Hasan, *Nature (London)* **460**, 1101 (2009).
- ²⁴Y. Zhang, C. Z. Chang, K. He, L. L. Wang, X. Chen, J. F. Jia, X. C. Ma, and Q. K. Xue, *Appl. Phys. Lett.* **97**, 194102 (2010).
- ²⁵C.-X. Liu, X. L. Qi, H. J. Zhang, Z. Dai, Z. Fang, and S. C. Zhang, *Phys. Rev. B* **82**, 045122 (2010).
- ²⁶H. Zhang, C. X. Liu, X. L. Qi, X. Dai, Z. Fang, and S. C. Zhang, *Nat. Phys.* **5**, 438 (2009).
- ²⁷D. Hsieh, Y. Xia, D. Qian, L. Wray, F. Meier, J. H. Dil, J. Osterwalder, L. Patthey, A. V. Fedorov, H. Lin, A. Bansil, D. Grauer, Y. S. Hor, R. J. Cava, and M. Z. Hasan, *Phys. Rev. Lett.* **103**, 146401 (2009).
- ²⁸G. Borstel, W. Borgiel, and W. Nolting, *Phys. Rev. B* **36**, 5301 (1987).
- ²⁹M. Barbagallo, N. D. M. Hine, J. F. K. Cooper, N. J. Steinke, A. Ionescu, C. H. W. Barnes, R. M. Dalgliesh, T. R. Charlton, and S. Langridge, *Phys. Rev. B* **81**, 235216 (2010).
- ³⁰P. Mahadevan, A. Kumar, D. Choudhury, and D. D. Sarma, *Phys. Rev. Lett.* **104**, 256401 (2010).
- ³¹J. M. An, S. V. Barabash, V. Ozolins, M. van Schilfgaarde, and K. D. Belashchenko, *Phys. Rev. B* **83**, 064105 (2011).